JOURNAL OF VIROLOGY, Sept. 2011, p. 8954–8967 Vol. 85, No. 17
0022-538X/11/$12.00 doi:10.1128/JVI.00754-11

Mechanism of Neutralization by the Broadly Neutralizing HIV-1 Monoclonal Antibody VRC01▽†

Yuxing Li,[1]‡ Sijy O'Dell,[1] Laura M. Walker,[2] Xueling Wu,[1] Javier Guenaga,[2] Yu Feng,[2] Stephen D. Schmidt,[1] Krisha McKee,[1] Mark K. Louder,[1] Julie E. Ledgerwood,[1] Barney S. Graham,[1] Barton F. Haynes,[3] Dennis R. Burton,[2] Richard T. Wyatt,[2]§* and John R. Mascola[1]§*

Vaccine Research Center, National Institute of Allergy and Infectious Diseases, National Institutes of Health, Bethesda, Maryland 20892[1]; IAVI Neutralizing Antibody Center at TSRI, Department of Immunology and Microbial Science, The Scripps Research Institute, La Jolla, California 92037[2]; and Duke University Medical Center, Durham, North Carolina 27710[3]

Received 14 April 2011/Accepted 20 June 2011

The structure of VRC01 in complex with the HIV-1 gp120 core reveals that this broadly neutralizing CD4 binding site (CD4bs) antibody partially mimics the interaction of the primary virus receptor, CD4, with gp120. Here, we extended the investigation of the VRC01-gp120 core interaction to the biologically relevant viral spike to better understand the mechanism of VRC01-mediated neutralization and to define viral elements associated with neutralization resistance. In contrast to the interaction of CD4 or the CD4bs monoclonal antibody (MAb) b12 with the HIV-1 envelope glycoprotein (Env), occlusion of the VRC01 epitope by quaternary constraints was not a major factor limiting neutralization. Mutagenesis studies indicated that VRC01 contacts within the gp120 loop D, the CD4 binding loop, and the V5 region were necessary for optimal VRC01 neutralization, as suggested by the crystal structure. In contrast to interactions with the soluble gp120 monomer, VRC01 interaction with the native viral spike did not occur in a CD4-like manner; VRC01 did not induce gp120 shedding from the Env spike or enhance gp41 membrane proximal external region (MPER)-directed antibody binding to the Env spike. Finally, VRC01 did not display significant reactivity with human antigens, boding well for potential *in vivo* applications. The data indicate that VRC01 interacts with gp120 in the context of the functional spike in a manner distinct from that of CD4. It achieves potent neutralization by precisely targeting the CD4bs without requiring alterations of Env spike configuration and by avoiding steric constraints imposed by the quaternary structure of the functional Env spike.

The HIV-1 envelope glycoprotein (Env) consists of the exterior gp120 and the transmembrane Env gp41, which comprise the functional trimer (10, 20, 21, 40, 54, 67, 68). The gp120 subunit interacts initially with the primary receptor, CD4, present on the surface of target cells (12, 30, 42). Receptor interaction results in substantial conformational changes in gp120, exposing the coreceptor binding site and permitting high-affinity binding to one of the coreceptors, either CCR5 or CXCR4 (1, 11, 13, 17, 19, 22, 63, 69). This receptor-and-coreceptor interaction triggers extensive rearrangements within gp41 (23, 29, 33, 60), which then mediates virus-to-target-cell membrane fusion and the entry of viral genomic information into susceptible target cells. During the course of natural infection, the HIV-1 Env elicits both type-specific and broadly cross-reactive neutralizing antibodies (24, 41, 50, 55, 66, 72). The latter response occurs in about 15% to 25% of HIV-1-infected individuals and can mediate neutralization of diverse viral isolates (14, 18, 37, 57, 61, 62). It has proven difficult to elicit such cross-reactive neutralizing antibody responses via Env immunization, in part due to the immune-dominance of gp120 variable regions and the apparent limited immune recognition of conserved regions of the viral Env (50, 72). To gain better insights that might apply to immunization strategies, investigators have focused on those HIV-1-infected individuals that mount neutralizing antibody responses to conserved regions of the viral Env (3, 14, 25, 37, 38, 57). Therefore, isolation of novel broadly neutralizing monoclonal antibodies (MAbs) and characterization of interactions with their cognate epitopes have received renewed interest.

Several broadly neutralizing monoclonal antibodies isolated from HIV-infected individuals define conserved epitopes on the HIV Env. These include the membrane proximal external region (MPER) of gp41, which is targeted by the MAbs 4E10, 2F5, and Z13 (5, 52, 75, 76), the carbohydrate-specific outer domain epitope which is targeted by 2G12 (5, 8, 56, 58, 64), a V2-V3-associated epitope which is targeted by PG9/PG16 (65), and the CD4 binding site (CD4bs) (7) targeted by several antibodies. The CD4bs overlaps with the conserved region on gp120, which is involved with engagement of CD4. The proto-

* Corresponding author. Mailing address for John R. Mascola: Vaccine Research Center, 40 Convent Drive, Bethesda, MD 20892. Phone: (301) 594-8487. Fax: (301) 480-2788. E-mail: jmascola@nih.gov. Mailing address for Richard T. Wyatt: The Scripps Research Institute, La Jolla, CA 92037. Phone: (858) 784-7676. Fax: (858) 784-7683. E-mail: wyatt@scripps.edu.

‡ Present address: IAVI Neutralizing Antibody Center, Department of Immunology and Microbial Science, The Scripps Research Institute, La Jolla, CA 92037.

§ These authors contributed equally.

† Supplemental material for this article may be found at http://jvi.asm.org/.

▽ Published ahead of print on 29 June 2011.

typical CD4bs-directed MAb b12 can neutralize ~40% of circulating primary isolates, and its structure in complex with the core of gp120 is defined (74). Interestingly, viral resistance to b12 only partially correlates with residue variation within the structurally defined epitope (71). Several b12-resistant viruses display an intact b12 epitope on their respective gp120 subunits (71), suggesting that quaternary packing of Env also confers resistance to b12. These observations emphasize that in addition to the structural information provided by X-ray crystallography of the antibody-Env interaction, phenotypic studies may provide additional insights into mechanisms of antibody-mediated neutralization and viral resistance.

We recently isolated three CD4bs-directed MAbs, VRC01, -02, and -03 (70), from a donor whose serum neutralization activity maps predominantly to the CD4bs (37). VRC01 and VRC02 are a closely related pair of somatic variants that neutralize over 90% of diverse HIV-1 primary isolates. The structure of VRC01 in complex with the gp120 core reveals that the VRC01 heavy chain binds to the gp120 CD4bs in a manner similar to that of the primary receptor, CD4 (73). However, the gp120 core lacks the major variable regions, as well as the N and C termini, and may only partially reflect the VRC01 interaction with full-length gp120, or with gp120 in the context of the native viral spike. In this study, we sought to further characterize VRC01 neutralization in the context of full-length gp120, its impact on the architecture of the viral Env functional spike upon binding, and viral factors associated with the relatively few cases of HIV-1 neutralization resistance.

MATERIALS AND METHODS

Generation of Env pseudovirus and neutralization assays. A panel of 119 JRCSF gp160 plasmid DNAs containing single point mutations in gp120 (51) or VRC01-resistant virus gp160 plasmid DNA was used in combination with a luciferase reporter plasmid containing the essential HIV structural genes to produce mutant Env pseudoviruses as described previously (35). In the case of making viruses treated with kifunensin, kifunensin (Cayman Chemical, Ann Arbor, MI) at 25 μM was added into the cell culture media 2 h before the transfection. The harvested cell culture supernatant containing the pseudovirus was stored at −80°C prior to use to perform either virus neutralization assays or enzyme-linked immunosorbent assay (ELISA)-based binding analysis. HIV-1 Env pseudoviruses were also used for neutralization assessment in a single round of an entry assay using TZM-bl target cells as previously described (35).

Env protein and antibody expression and purification. HIV-1 gp120 was expressed in *Drosophila* S2 cells and purified with 17b-coupled protein A affinity columns as previously described (38). Antibody 2G12 was obtained from Polymun Scientific, Inc. (Vienna, Austria). Four-domain soluble CD4 (D1 to D4) of CD4 was purchased from Progenics (Tarrytown, NY). The plasmid encoding CD4-Ig contains the D1D2 domain fused with the human Fc fragment was provided by Joseph Sodroski (Dana Farber Cancer Institute) and used to transfected 293 FreeStyle cells as previously described to express CD4-Ig secreted into cell culture supernatant (38), followed by purification with a protein A affinity column (GE Healthcare). IgG b12 has been described previously (7). V3 region-specific 447D was provided by Susan Zolla-Pazner (New York University CFAR), and the CD4i antibodies 17b, 48D, 2.1c, and A32, along with the C1/C5 conformational antibody C11, were provided by James Robinson (Tulane University).

gp120 and CD4bs ligand-binding ELISA. MAb and CD4 binding to monomeric gp120 dissociated from Env pseudovirus proteins was measured using antibody capture and evaluated by sandwich ELISA as previously described (43), with minor modifications (71). Relative affinities (avidities) were calculated as the antibody concentration at half-maximal binding (50% effective concentration [EC_{50}]) derived by curve fitting with software GraphPad Prism, version 5.0 (GraphPad Software Inc., La Jolla, CA) using the sigmoidal dose-response model with a variable slope. 2G12 binding to virus monomeric gp120 was used to normalize the amount of virus gp120 in each virus lysate preparation. In cases of poor 2G12 recognition of gp120 due to 2G12 epitope mutations, such as N332A, HIV-Ig, or MAb 447, was used for normalization. The effect of a given mutation on antibody binding was represented by apparent affinity (avidity) relative to those for wild-type (WT) gp120, calculated with the formula ([(EC_{50}_WT/EC_{50}_mutant)/(EC_{50}_WT for 2G12/EC_{50}_mutant for 2G12)] × 100). Competition ELISAs of biotin-labeled antibodies were carried out with recombinant YU2 gp120 captured in ELISA wells coated with the sheep D7324 polyclonal antibody, which is specific for the gp120 C5 region as described previously (70).

ITC. Isothermal titration calorimetry (ITC) measurements were carried out by using the ITC200 microcalorimeter system (MicroCal, Inc.). All reactions were performed at 37°C as previously described (70). The concentration of gp120 in the sample cell was approximately 5 μM, and that of CD4-Ig, VRC01, or 17b in the syringe was approximately 50 μM. The molar concentrations of the proteins were calculated using the following molar extinction coefficients: gp120, 1.52; VRC01, 1.53; CD4-Ig, 1.20; and 17b, 1.36. For the second step of a two-step reaction, the gp120 concentration was recalculated per the final volume at the end of the first reaction, which is equal to the sample cell volume plus the total volume of the first injectate. Before the second titration, the sample volume equivalent to the volume of the first injectate was removed from the sample cell. Data were analyzed with Microcal ORIGIN software using a single-site binding model.

HIV-1 Env gp120 shedding. 293T cells were transfected with the full-length JRFL or JRCSF Env-expressing plasmid pSVIII as described previously (49). Forty-eight hours posttransfection, approximately 2×10^7 cells were collected, washed with PBS, and concentrated to 1×10^7cells/ml. Two-hundred-microliter aliquots of the cell suspension were deposited into microcentrifuge tubes for each ligand at a given concentration. The tubes containing the cells were subjected to a 5-min centrifugation at 335 × *g* at room temperature to pellet the cells. A total of 160 μl of the supernatant was removed and discarded. A total of 20 μl of the ligand solution prepared in a serial dilution was added to the cell pellets, and following mixing, the cells and ligand were incubated at 37°C for 1 h with gentle mixing every 20 min. The cells were then subjected to centrifugation, and the supernatants were transferred to fresh tubes. A total of 30 μl of each supernatant was loaded onto SDS-PAGE gels and run for 1.5 h at 200V. The proteins were transferred to nitrocellulose membranes for Western blotting. To identify gp120, the V3-specific anti-gp120 human monoclonal 39F was used as a primary antibody (1 μg/ml), followed by a horseradish peroxidase (HRP)-conjugated anti-human secondary antibody (Jackson ImmunoResearch Laboratories, West Grove, PA) at a 1:10,000 dilution, and development with substrate followed.

Antibody self-antigen recognition assays. Two assays were used for evaluation of the MAb reactivity to self-antigens as previously described (27). Briefly, the luminex AtheNA Multi-Lyte ANA test (Wampole Laboratories, Princeton, NJ) was used to test for MAb reactivity to self antigens: systemic lupus erythematosus autoantigens SSA and SSB, sphingomyelin (Sm), ribonucleoprotein (RNP), sclerosis autoantigen (Scl-70), histidine-tRNA ligase (Jo-1), double-stranded DNA (dsDNA), and centromere B (CentB). Reactivity to HIV-1-negative human epithelial HEp-2 cells was determined by indirect immunofluorescence on HEp-2 slides using Evans Blue as a counterstain and fluorescein isothiocyanate (FITC)-conjugated goat anti-human IgG (Zeus Scientific, Raritan NJ). Antibody reactivity with phospholipid was assessed with activated partial thromboplastin time (aPTT) automated reagent (Diagnostica Stago, Parsippany, NJ), and time to clot formation was measured as an indicator of phospholipid reactivity. Anti-respiratory syncytial virus (RSV) monoclonal antibody, Synagis (palivizumab; MedImmune, MD) and plasma from normal donors were used as negative controls.

RESULTS

Characterization of VRC01 binding and neutralization specificity using a panel of Env alanine mutants. The previously published crystal structure of VRC01 in complex with a monomeric gp120 core revealed the antibody contact sites on the trimmed protein lacking the major variable regions V1, V2, and V3 and portions of the N and C termini (73). To study the VRC01 interaction with the functional viral spike, we used a panel of JRCSF alanine (Ala) scanning Env pseudovirus mutants (51) to assess the neutralization potency of VRC01 in comparison to that of CD4-Ig and the prototypic CD4bs MAb b12 (Fig. 1). Since some of the JRCSF Env mutants were not entry competent, we also studied VRC01 binding to Ala scan-

			gp120 contact with mAbs			Neutralization sensitivity relative to WT (%)			Binding affinity relative to WT (%)				
	gp120 domain	gp120 mutation	VRC01	CD4	b12	VRC01	CD4-Ig	b12	VRC01	CD4-Ig	b12	2G12	447D/ HIVIg
		WT				100	100	100	100	100	100	100	100
Inner domain	C1	E87A				63	46	29	98	92	303	100	110
		M95A				56	17	48	82	108	43	100	91
		K97A	*			62	184	117	88	117	125	100	63
		E102A				98	60	83	100	100	100	100	100
		W112A				78	100	119	105	108	744	100	46
	C1 (bridging sheet, V1V2 stem)	V120A				60	161	80	145	122	564	100	120
		K121A				24	28	30	113	168	601	100	92
		L122A				66	474	96	104	110	529	100	107
		L125A		●		222	9532	1549	ND	ND	ND	ND	ND
		V127A		●		ND	ND	ND	160	108	763	100	79
		N156A†				68	>10000	2345	ND	ND	ND	ND	ND
		N160K				296	99	173	104	108	115	100	3
	V2	T162A				190	318	107	ND	ND	ND	ND	ND
		I165K				42	434	41	102	110	231	100	93
		I165A				ND	ND	ND	125	157	588	100	64
		R166A				42	22	41	117	168	300	100	91
		D167N				99	702	121	125	87	14	100	93
		K171A				50	106	80	135	152	322	100	107
		E172A				60	52	58	134	158	169	100	93
		F176A				161	259	55	93	54	161	100	118
		Y177A				89	>10000	2416	153	136	165	100	76
		L179A				13	1526	19	171	160	154	100	71
		D180A				ND	ND	ND	109	74	375	100	119
		V182A				60	128	45	ND	ND	ND	ND	ND
		I184A				129	806	172	141	94	227	100	100
		D185A				34	96	4	113	61	1080	100	74
		T190A				119	8	165	103	128	269	100	53
	C2 Bridging sheet (V1V2 stem)	N197A†				ND	ND	ND	72	45	81	100	42
		N197K†				ND	ND	ND	93	34	73	100	123
		N197T†				ND	ND	ND	75	20	23	100	121
		T198A				40	218	5	ND	ND	ND	ND	ND
		S199A†				724	2903	5973	118	57	100	100	148
		T202A				30	3831	569	102	140	192	100	30
	C2 β3a	F210A				163	845	384	121	128	650	100	81
		I213A				174	102	178	97	104	237	100	66
Outer domain	C2 Loop B	R252A				ND	ND	ND	121	105	409	100	107
		R253A				68	21	98	ND	ND	ND	ND	ND
		S256A			○	73	112	83	82	133	390	100	116
		T257A			●	253	5	107	39	51	167	100	103
		N262A†				223	63	443	35	6	189	100	155
	C2 Loop D	R273A				48	132	109	59	130	91	100	119
		N276A†	*			341	29	134	193	107	71	100	113
		D279A	●	●		3	2	92	0	58	41	100	111
		N280A	●	●	●	ND	ND	ND	66	81	212	100	85
		K282A	*	●		363	5	78	68	86	124	100	108
		T283A	*	●		346	5	717	78	106	98	100	97
	V3 (base)	N295A†				56	46	85	ND	ND	ND	ND	ND
		T297S				50	17	47	94	109	101	100	97
		R298A				ND	ND	ND	114	254	427	100	116
		N301A†				239	8163	1396	142	171	191	100	130
	V3 (stem)	N302A				43	28	75	ND	ND	ND	ND	ND
		R304A				32	4497	125	150	256	104	100	137
		K305A				70	>10000	3466	153	146	164	100	64

FIG. 1. VRC01 neutralization and binding on a panel of primary isolate JRCSF functional Env and gp120 mutants. Amino acid numbering of mutants is based on the HIV-1 HXBc2 sequence. The gp120 structurally defined contact residues for the VRC01, CD4, and b12 complexes are indicated in blue, orange, and green, respectively, with open circles (○) designating gp120 main-chain-only contacts, asterisk (*) designating gp120 side chain-only contacts, and filled circles (●) designating both main-chain and side-chain contacts. Mutations that knock out putative N-glycosylation sites (NXS/T motifs) of gp120 are labeled with a dagger symbol (†). Relative ELISA binding affinities to captured gp120s were calculated based on the antibody concentration at half-maximal binding (EC_{50}). The effect of each mutation on antibody binding was normalized using 2G12 to control for the amount of captured gp120. Mutations that resulted in decreased gp120 binding (<33% relative to that of wild type [WT]) are highlighted in blue, and those that resulted in increased ELISA binding (>300% relative to that for the wild type) are highlighted in red. HIVIg or the anti-V3 MAb 447D (values shown in red) were used as the controls for gp120s with poor 2G12 binding. Neutralization sensitivity of each mutant to MAb VRC01, CD4-Ig, or MAb b12 was assessed and compared to neutralization of the wild-type Env pseudovirus. The color scheme is the same as that used for the gp120 binding data.

				gp120 contact with mAbs			Neutralization sensitivity relative to WT (%)			Binding affinity relative to WT (%)				
	gp120 domain		gp120 mutation	VRC01	CD4	b12	VRC01	CD4-Ig	b12	VRC01	CD4-Ig	b12	2G12	447D/ HIVIg
			WT				100	100	100	100	100	100	100	100
	V3 (tip)		S306A				76	246	94	94	75	97	100	133
			I307A				119	>10000	7399	155	206	142	100	253
			H308A				66	505	76	194	222	137	100	126
			I309A				82	>10000	3493	66	193	166	100	17
			P313A				130	3	13	91	138	122	100	149
			R315A				45	393	67	114	134	173	100	109
			R315Q				ND	ND	ND	154	239	203	100	149
			F317A				116	>10000	4709	155	134	173	100	73
			Y318A				109	>10000	4846	167	144	185	100	76
			T319A				56	316	54	98	123	149	100	92
			T320A				56	>10000	1240	130	163	295	100	142
	V3 (base)		E322A				110	293	76	116	106	123	100	75
			D325A				53	444	154	118	233	304	100	91
			A329K				ND	ND	ND	303	983	0	100	300
			H330A				ND	ND	ND	116	109	55	100	91
			N332A†				119	118	143	60	32	47	1	100
	C3	α2	Q337A				43	20	56	101	165	164	100	191
			K343A				45	34	65	105	177	103	100	108
			R350A				60	21	76	108	232	234	100	102
		CD4 binding loop	S364A			✱	ND	ND	ND	259	122	148	100	109
			S365A	●	●	●	114	32	70	149	150	216	100	115
			G366A	○	○	○	ND	ND	ND	50	68	15	100	175
			G367A	○	○	○	ND	ND	ND	28	23	23	100	144
			D368A	●	●	●	ND	ND	ND	3	0	0	100	137
			P369A		✱	●	72	26	30	120	177	343	100	143
			E370A		✱	●	ND	ND	ND	27	25	29	100	77
			I371A	✱		●	ND	ND	ND	30	33	37	100	106
			V372A			✱	74	12	12	63	220	11	100	113
			M373A			✱	90	37	124	83	166	1008	100	133
			Y384A			●	ND	ND	ND	43	127	126	100	50
			N386A†			●	212	50	392	212	375	449	100	83
			T388A				196	110	482	106	141	324	100	139
Outer domain	V4		N392Q†				44	29	63	ND	ND	ND	ND	ND
			W395A				ND	ND	ND	181	224	53	100	449
	C4	β19	R419A			●	120	596	30	133	194	283	100	137
			I420A				16	1015	344	118	193	215	100	71
			K421A				64	>10000	1457	133	175	151	100	60
			Q422A				47	5369	657	ND	ND	ND	ND	ND
			I423A				19	>10000	3412	260	439	356	100	87
		Bridging sheet (β20/21 hair pin)	I424A				26	>10000	2301	205	425	203	100	120
			N425A		●		61	22	98	73	158	144	100	91
			W427A	○	●		ND	ND	ND	76	134	108	100	96
			V430A	✱	●	●	36	>10000	4336	98	146	697	100	93
			K432A		✱	✱	55	147	61	90	240	494	100	165
			Y435A			✱	31	3407	2034	96	212	830	100	130
			I439A				162	2854	656	129	288	903	100	181
			T450A				84	31	126	52	68	53	100	141
		β23	T455A	✱	✱	✱	79	22	27	65	137	69	100	76
			R456A	●	○	○	63	55	106	80	102	51	100	129
			D457A	●	●	●	ND	ND	ND	29	8	20	100	89
			G458A	○	○	○	ND	ND	ND	84	51	94	100	71
			G459A	○	○		149	722	69	63	63	104	100	100
	V5		N461A†	●			363	97	90	306	172	201	100	89
			E462A				46	38	49	ND	ND	ND	ND	ND
			S463A†	✱			536	54	109	267	97	133	100	141
	β24		I467A	●			ND	ND	ND	28	93	65	100	132
			R469A	✱	✱		ND	ND	ND	62	11	357	100	154
	C5	β24-α5 connection	G471A		○	○	25	10	70	107	111	56	100	212
			G472A	○	○	○	ND	ND	ND	84	7	133	100	114
			G473A	○	○	○	ND	ND	ND	79	0	97	100	63
			D474A	●	●	●	32	11	109	20	29	406	100	120
			M475A		✱	●	68	61	59	ND	ND	ND	ND	ND
			R476A	✱	✱		200	5	129	55	66	398	100	82
			D477A		✱		68	10	158	51	91	147	100	163
			W479A				160	70	508	70	63	303	100	105
			R480A				200	53	150	110	230	557	100	69

FIG. 1—*Continued*.

ning mutants in the context of full-length monomeric JRCSF gp120. Consistent with the structural analysis, the mutational analyses confirmed that mutations at residues in loop D (N terminal to the V3 region), the CD4 binding loop, and the V5-β24-α5 region diminished VRC01-mediated binding or neutralization (Fig. 1). In some cases, single mutations, such as D279A (loop D) and D474A (β24-α5), diminished both VRC01-mediated neutralization and binding to the corre-

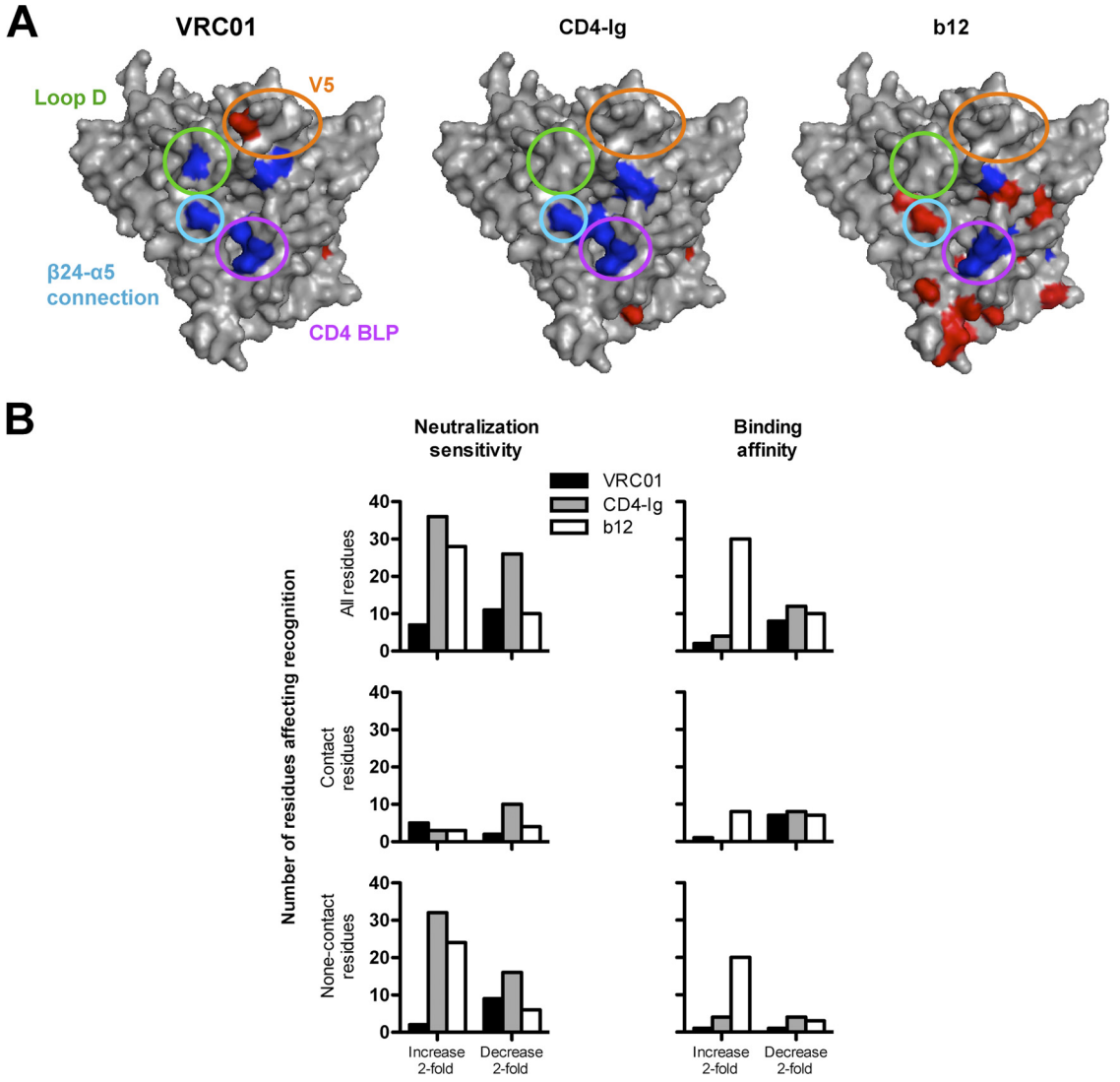

FIG. 2. (A) Surface model of the JRCSF gp120 core showing mutants resulting in decreased binding (blue) or increased binding (red). The gp120 domains that contain mutations most affecting affinities for VRC01 are denoted in circles of the following colors: green, loop D; gold, V5/β24; purple, CD4 BLP (CD4 binding loop); and blue, β24-α5 connection. (B) Histograms showing the number of mutant residues affecting virus neutralization or gp120 binding for VRC01, b12, and CD4-Ig.

sponding gp120. For other contact sites, such as those in the CD4 binding loop, neutralization could not be tested since these Envs did not support entry, but Ala mutations at G367, D368, and I371 resulted in diminished binding to gp120. However, for many of the predicted contact sites, individual Ala mutations did not result in a measurable decrease in either VRC01 binding or neutralization. This is perhaps not surprising, as single residue mutations may be insufficient to disrupt high-affinity antibody-ligand binding if the specific contact does not contribute substantial binding energy to the ligand-ligand interaction. In addition, the energetics of binding contributed by individual residues is not always fully evident from the structurally defined protein-protein interface alone. Of note, gp120 loop D and V5 regions contained substitutions uniquely affecting VRC01 binding, but not b12 or CD4-Ig binding (Fig. 2A).

We also observed that Ala mutations beyond the structurally defined VRC01, CD4, and b12 contact sites and scattered within V2, V3, the bridging sheet, and β19 regions significantly affected neutralization sensitivity to these CD4bs ligands (Fig. 1). In most cases, these mutations had more pronounced effects on viral neutralization than on monomeric gp120 binding affinity, suggesting effects on functional spike quaternary interactions or "packing" (9). In a few cases, Ala mutations at such "noncontact" residues diminished neutralization by b12, CD4-Ig, or VRC01 (e.g., K121A and L179A). However, in most cases, these mutations resulted in a marked enhancement of viral neutralization sensitivity, especially for ligands CD4-Ig and b12. Specifically, mutations located in V2 (L179A) and V3 (R304A) and clustered in the bridging sheet (S199A, T202A, I424A, and Y435A) and β19 (I420A and I423A) facilitated increases in CD4-Ig or/and b12 neutralization potency while imbuing VRC01 potency with less quantitative increases (Fig. 1). A few mutations that eliminated N-glycosylation sites in the

V1V2 stem (S199A), loop D (N276A), or V5 (N461A or S463A) resulted in enhanced VRC01 potency (Fig. 1). Perhaps these Ala substitutions better expose the VRC01 epitope in the spike context as most of these mutations had a minor effect on binding affinity to the gp120 monomer. Overall, the Ala scanning mutagenesis data revealed that there were many more noncontact mutations leading to increased viral neutralization sensitivity for CD4-Ig and b12 than for VRC01, especially in the major variable regions V1, V2, and V3 (Fig. 2B).

Steric hindrance is not a major factor limiting VRC01 neutralization. It has previously been reported that limitations to antibody access to the CD4bs may restrict neutralization by CD4bs antibodies, including the neutralizing MAb b12 (4, 31, 32, 36). This steric hindrance is thought to be a result of the three-dimensional structure of the functional viral spike, including packing of the variable loops and N-linked glycan shielding. Thus, viral resistance to b12 can often occur due to limitations of the antibody access to the CD4bs, even when the MAb cognate contact residues are present on a given gp120 (71). Since VRC01 can neutralize approximately 90% of virus isolates by precisely targeting the CD4bs (70), we hypothesized that access to the CD4bs may not be a major restriction to its neutralization breadth. Stated in another way, neutralization by VRC01 should correlate closely with gp120 binding affinity, and few mutations on the Env glycoprotein should result in increased binding or neutralization by VRC01. This hypothesis is consistent with our neutralization and binding results conducted with the JRCSF mutant virus panel shown in Fig. 1. Here, to extend the analysis with more circulating virus strains and various Env regions, we also evaluated the impact of previously described mutations that alter the Env structure or neutralization sensitivity and which also result in an increased neutralization potency by either MAb b12 or by CD4-Ig. Removal of a V3 loop N-linked glycan at position 301 (via a T303A mutation) (31) or mutations in gp41 (T569A/I675V) (4) resulted in marked enhancement in the potency of neutralization by b12 and CD4-Ig, but these mutations did not significantly affect VRC01-mediated neutralization (Fig. 3A).

Taken together, these results described immediately above, along with the JRCSF Ala virus mutant panel data, suggest that VRC01 can approach its cognate epitope on the functional spike with less steric hindrance than does b12 and, surprisingly, with less hindrance than the soluble form of the virus receptor CD4 itself (Fig. 3B). These differences might be related to the quite different angle of approach to the CD4bs employed by VRC01, in contrast to the more loop-proximal approach employed by CD4 and b12 (see the trimer model for these ligands shown in Fig. 3B).

Further analysis of 16 VRC01-resistant viral isolates (from a panel of 190) (70) showed that VRC01 bound poorly to gp120 C5-specific antibody-captured gp120 derived from 15/16 primary isolate viruses (Table 1). VRC01 demonstrated relatively strong binding to the captured gp120 of only one neutralization-resistant virus, 3817_V2_C59. This is in contrast to our previous finding for b12, in which b12 bound with high relative affinity to eight of the 14 b12-resistant viral gp120s (71). Taken together, these data demonstrate that the relatively infrequent cases of VRC01 natural resistance arise largely from antigenic variation at the direct gp120 contact site itself, rather than by steric restrictions on access to the CD4bs that is more commonly observed for naturally occurring b12 resistance. These data are consistent with the Env functional spike model shown in Fig. 3B, in which V loop packing impacts b12 access to its epitope to a greater degree than it does VRC01 epitope access.

Antigenic and sequence variation of gp120 displayed by VRC01-resistant viruses. Our prior analysis of the sequence of 17 VRC01-resistant isolates, based upon the structurally defined contact sites of VRC01 on the gp120 core, demonstrated that the most resistant isolates contained alterations in residues in one of two regions of gp120: loop D or the V5 region (73) (see Fig. S1 in the supplemental material). In addition to these two sites, we also observed primary amino acid sequence variation within the CD4 binding loop region (see Fig. S1 in the supplemental material). In contrast, the gp120 of most VRC01-sensitive viruses contained intact VRC01 contact sites. Specifically, sequence variation was located within a 5-amino acid motif of ^{278}T(D/N)NAK^{283} of loop D, within residues 362 to 365 of the CD4 binding loop and flanking potential N-linked glycosylation, and within residues 458 to 467 of the V5/β24 region. One interpretation of these observations is that the motif variations are linked, suggesting that multiple alterations in more than one of the gp120 hotspots might be required to generate full VRC01 neutralization resistance. For example, the resistant virus 242-14 contains variations in the CD4 binding loop and in V5/β24; and the resistant isolate, T278_50, possessed variations in both loop D and V5.

To test the hypothesis that multiple changes in the described motifs contribute to full VRC01 resistance, we altered specific residues and made chimeric "swaps" to restore VRC01-sensitive viral sequences (e.g., that of the reference virus Env from HXBc2) to these resistant viruses (Table 2). We selected five viruses with the typical features of variation described above and tested this hypothesis, as described below.

For resistant virus 242-14, full sensitivity to VRC01 was restored by a set of mutations that included a V5 swap, a V5/β24 A467I mutation, and replacement of residues flanking the CD4 binding loop with wild-type HXBc2 sequences. Individual mutations were insufficient to produce a sensitive virus, whereas the full set of mutations resulted in both high binding to the captured gp120 and potent neutralization (Fig. 4A; Table 2). These data suggest that each single alteration restores VRC01 recognition to a degree, but all are required for full sensitivity.

Similarly, the viral isolate T278-50 contained variations from gp120s derived from VRC01-sensitive viruses in both the loop D region (residue A279) and the V5 region (residue E459). Altering both sites to the wild-type sequence was required to restore VRC01 binding to gp120 and to recover full sensitivity to VRC01-mediated neutralization (Fig. 4A; Table 2). In addition, the viral isolates BL01 and TV1_29 both contained variations in the structurally defined VRC01 contact sites in loop D, in the CD4 binding loop, in the V5 region, and in the β24-α5 connection (see Fig. S1 in the supplemental material). Restoring the loop D residues, CD4 binding loop residues, and the V5 region residues to VRC01-sensitive viral sequences restored both VRC01 binding to gp120 and sensitivity to VRC01-mediated neutralization (Table 2), strongly suggesting that the aforementioned resistance motifs within gp120 contribute to the VRC01-resistant phenotype of these isolates. We also performed mutagenesis on isolate 57128_02, which dis-

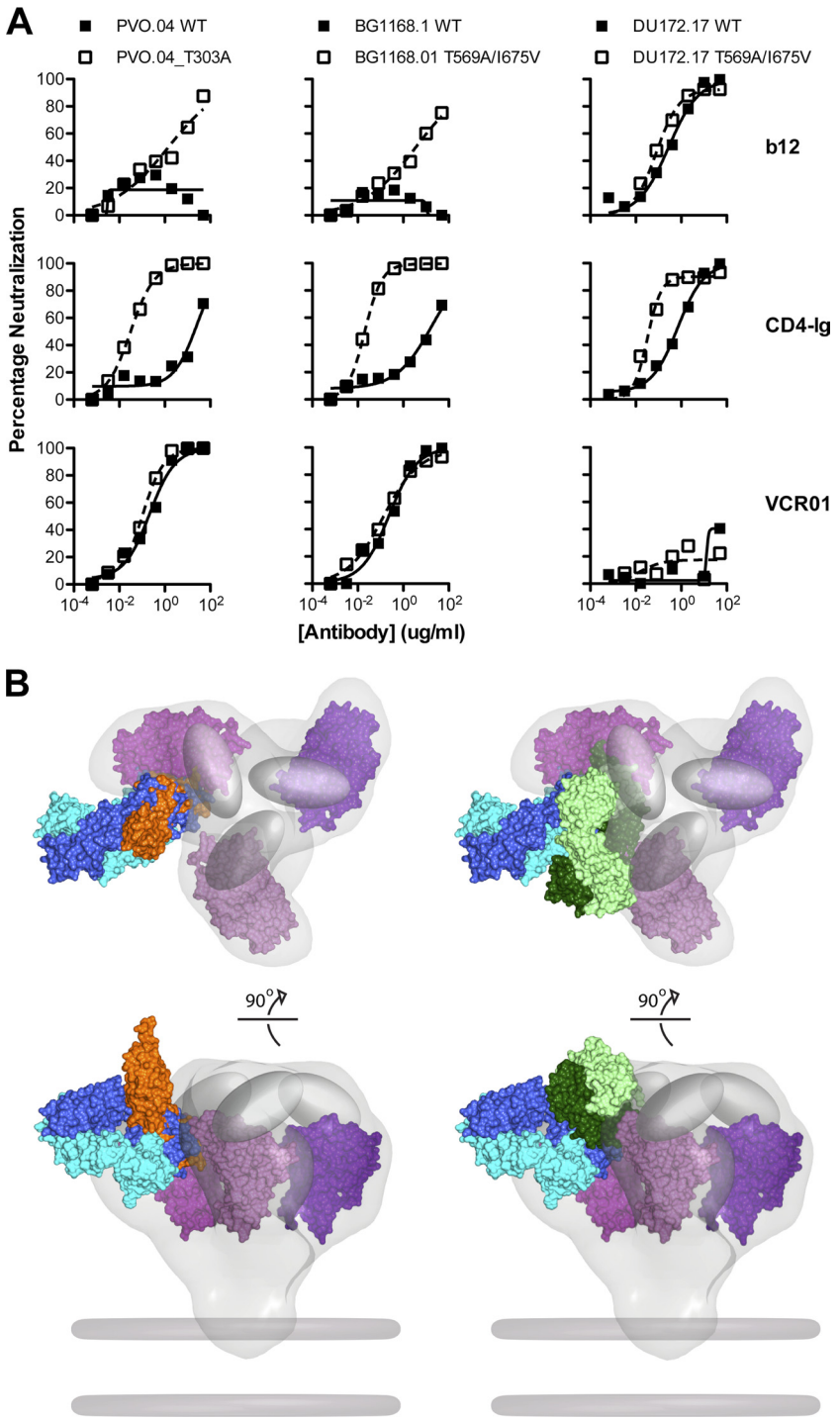

FIG. 3. Impact of conformational constraints on neutralization by b12, CD4-Ig, and VRC01. (A) Env pseudoviruses PVO.04 (left) and BG1168.1 (middle) are relatively resistant to b12 and CD4-Ig. In the setting of the gp120 T303A mutation or the gp41 T569A/I675V mutations that result in a more open Env conformation, these viruses show enhanced neutralization sensitivity to b12 and CD4-Ig. In contrast, both the wild-type and mutant versions of these viruses were equally sensitive to VRC01-mediated neutralization. Virus DU172.17 (right) was resistant to VRC01, and this resistance was not affected by the Env mutations that alter conformation. (B) Model of VRC01, CD4, and b12 binding to the HIV-1 functional spike. Top (top) and front (bottom) views of the density map surface of the HIV-1 spike, presenting three gp120 core protomers in magenta (39) (Electron Microscopy Database [EMDB]: EMD-5019; Protein Data Bank [PDB]: 3DNN) and viral membrane in dark gray. To analyze the relative binding orientations of b12, CD4, and VRC01, the X-ray coordinates for gp120, in the b12, VRC01, and CD4/17b/bound conformations (PDB: 2NY7, 3NGB, and 2NY3), respectively, were superimposed on the same gp120 core protomer (PDB: 3DNN). The molecular surface of the b12-Fab fragment is green; the VRC01 Fab is blue. Within each color-coded Fab, the heavy chains are shaded darker than the light chains. The molecular surface of sCD4 is orange, and the variable loops are represented as gray ovals. Note that in this model, b12 and CD4 are more loop proximal than is VRC01.

TABLE 1. VRC01-resistant virus binding/neutralization profile

Clade	Virus	VRC01		b12		CD4-Ig		F105	2G12	HIV-Ig
		B-EC$_{50}$[a]	N-IC$_{50}$[b]	B-EC$_{50}$	N-IC$_{50}$	B-EC$_{50}$	N-IC$_{50}$	B-EC$_{50}$	B-EC$_{50}$	B-EC$_{50}$
B	AY124970_BL01	>50	>50	0.1	1.7	0.01	0.1	>50	0.3	0.7
B	EF210732_HO86_8	>50	>50	>50	>50	0.006	9.8	ND	0.4	0.2
C	CAP210_2_00_E8	>50	>50	0.03	27	0.4	1.5	>50	5.5	0.7
C	DU172-17	>50	>50	0.01	0.3	0.03	0.3	>50	7.5	0.4
C	DU422_1	>50	>50	2	0.46	24.4	11.5	>50	1.1	1.2
C	TV1_29	>50	>50	>50	>50	19	0.4	>50	1	4.5
C	TZA125_17	>50	>50	>50	>50	0.02	0.1	0.06	0.9	0.4
D	57128_02	8.7	>50	0.001	0.17	0.04	0.1	0.003	0.03	0.4
G	EU885764_X2088_9	>50	>50	>50	>50	0.03	2.4	0.3	0.3	0.2
CRF02_AG	242-14	>50	>50	>50	>50	0.001	1.9	0.01	0.3	0.2
CRF02_AG	T250-4	>50	>50	>50	>50	0.011	6	>50	0.03	0.2
CRF02_AG	T278-50	>50	>50	0.01	18.4	0.001	1.6	>50	0.7	0.01
CRF01_AE	620345_C1	>50	>50	0.01	>50	0.002	>50	>50	0.3	0.2
recombinant	3817_V2_C59	0.04	>50	0.003	>50	0.001	>50	0.006	0.003	0.1
recombinant	6540_V4_C1	>50	>50	>50	16.1	0.002	3.7	ND	0.2	1.1
recombinant	6545_V4_C1	>50	>50	0.006	31.5	0.003	3	0.3	0.2	0.8

<1ug/ml
1-50 ug/ml
>50ug/ml

[a] B-EC$_{50}$ (μg/ml), half-maximal effective concentration of ELISA binding assay.
[b] N-IC$_{50}$ (μg/ml), 50% inhibitory concentration of neutralization assay.

plays variability at residue 283 (I283T) in loop D, in residues 362 to 365 of the CD4 binding loop, and in the V5-β24 region (Table 2). Reversion to putative VRC01 contact sequences in these three regions resulted in a gp120 with restored VRC01 binding recognition and a virus displaying moderate VRC01-mediated neutralization sensitivity (Fig. 4B; Table 2).

It is of note that, with the exception of the TV1-29 isolate, all the VRC01 neutralization reversion mutants are more resistant to HIV-Ig neutralization (Table 2). This might be explained by the likely possibility that the majority of the neutralization specificity in HIVIG, a pool of IgGs derived from HIV-1-infected individuals, is distinct from that of the monospecific VRC01 MAb.

As noted above, VRC01 bound with high relative affinity (avidity) to the monomeric gp120 of only one resistant isolate, 3817_V2_C59. Sequence analysis indicated that the structurally defined VRC01 epitope on this gp120 was intact and, as opposed to the 15 other cases, that resistance might be due to indirect conformational influences resulting in occlusion of the VRC01 epitope in the context of the viral functional spike. To test this possibility, we generated a 3817_V2_C59 Env pseudovirus in the presence of kifunensin. Kifunensin treatment of the viral producer cells inhibits formation of complex N-glycans on the viral Env (2, 16, 59). Compared to the virus generated from untreated cells, the kifunensin-treated virus was more sensitive to VRC01-mediated neutralization (Fig. 4B; Table 2). Thus, in this one case, viral resistance to VRC01-mediated neutralization was likely due to a glycan-dependent limitation of VRC01 accessibility to its epitope in the context of the functional Env spike.

VRC01 and CD4 interaction with gp120 displays differential effects on the coreceptor binding site. Previously, we demonstrated that VRC01 induced substantial conformation changes upon binding to monomeric gp120, as assessed by isothermal titration calorimetry (ITC) (70), in a manner very similar to that displayed by sCD4 interacting with gp120 (47). Here, we more fully characterized the effects of VRC01 binding to gp120, compared to those of the viral receptor CD4 and the coreceptor mimetic MAb 17b. We did this comparison by performing a complete thermodynamic cycle analysis using VRC01 and CD4-Ig in parallel, along with 17b (Fig. 5A). The change in enthalpy (ΔH) and entropy ($-T\Delta S$) of gp120 upon binding to the CD4bs or coreceptor binding site ligands was determined. These thermodynamic values are thought to reflect conformational changes imposed by the binding of each of these gp120 ligands. As reported previously, following gp120 interaction with CD4-Ig, VRC01, or 17b, individually, gp120 undergoes a large conformational change as assessed by the observed large change in enthalpy (~50 kcal/mol for both CD4 and VRC01) (Fig. 5B). However, when CD4-Ig or VRC01 was mixed with gp120 to form stable complexes prior to the addition of 17b, the change in enthalpy of 17b binding to gp120 was reduced more than 50% compared to the 17b-gp120 ΔH value, without the prior addition of either CD4-Ig or VRC01 (Fig. 5B). These data are consistent with the previous observation that both CD4 and VRC01 can stabilize monomeric gp120 in a 17b-preferred binding conformation. Although VRC01 induction of the 17b epitope was slightly less than that of CD4, the overall signatures comprised by the full thermodynamic cycles derived from these ligands were quite similar (Fig. 5B).

To further characterize the effects of the VRC01-gp120 interaction on coreceptor-directed antibodies as a class, we analyzed the impact of gp120 recognition by CD4i antibodies not previously evaluated. Recognition of these antibodies to gp120 was assessed in the presence or absence of the positive control, CD4-Ig, or the VRC01 MAb. The CD4i MAb 48D displayed

TABLE 2. VRC01-resistant virus reversion mutant mutagenesis and binding/neutralization profile[c]

Virus	Env sequence			Tested antibodies							
				VRC01		b12		CD4-Ig		HIVIG	
	Loop D (276-283)	CD4 BLP (362-374)	V5/β24 (458-469)	B-EC$_{50}$[a]	N-IC$_{50}$[b]	B-EC$_{50}$	N-IC$_{50}$	B-EC$_{50}$	N-IC$_{50}$	B-EC$_{50}$	N-IC$_{50}$
HXBc2	NFTDNAKT	KQSSGGDPEIVTH	GGNSNNESE IFR	0.024	0.04	0.005	0.007	0.0036	0.005	0.53	18.4
JR-CSF	NFTDNAKT	THSSGGDPEIVMH	GGKNESEIE IFR	0.11	0.093	0.011	0.096	0.034	0.186	0.18	123
93TH057	NLTNNAKT	QPPSGGDLEITMH	GGANNTSNE TFR	ND	ND	ND	ND	ND	ND	ND	ND
242-14.WT	NISNNGKT	TNHSGGDLEVTTH	GGFRNDTNETYEAFR	>50	>50	>50	>50	0.001	1.5	0.2	638
242-14.A467I	NISNNGKT	TNHSGGDLEVTTH	GGFRNDTNETYEIFR	>50	>50	>50	>50	0.002	0.6	0.9	1017
242-14.V5 Swap	NISNNGKT	TNHSGGDLEVTTH	GGNSNNESE EAFR	>50	>50	>50	>50	0.02	1.3	9.0	836
242-14.V5 Swap/A467I	NISNNGKT	TNHSGGDLEVTTH	GGNSNNESE IFR	13.8	>50	>50	>50	0.002	0.2	215.3	1435
242-14.CD4 BLP mut (N363Q/H364S)	NISNNGKT	TQSSGGDLEVTTH	GGFRNDTNETYEAFR	>50	>50	0.02	>50	0.001	0.5	0.5	241
242-14.CD4 BLP mut/V5 Swap/A467I	NISNNGKT	TQSSGGDLEVTTH	GGNSNNESE IFR	0.01	0.9	0.003	>50	0.001	0.2	0.5	1580
T278-50.WT	NISANAKT	TKPSGGDLEITTH	GEGDEKANE TFR	>50	>50	0.01	28	0.001	1.6	0.01	3012
T278-50. Loop D mut (A279D)	NISDNAKT	TKPSGGDLEITTH	GEGDEKANE TFR	10.3	>50	0.05	6.66	0.01	0.5	2.1	>5000
T278-50.V5 mut (E459G)	NISANAKT	TKPSGGDLEITTH	GGGDEKANE TFR	>50	>50	0.2	22	0.2	1.8	4.9	572
T278-50.Loop D/V5 mut(A279D/E459G)	NISDNAKT	TKPSGGDLEITTH	GGGDEKANE TFR	0.9	4.6	0.05	30	0.02	0.3	5.4	>5000
T278-50.V5 Swap	NISANAKT	TKPSGGDLEITTH	GGNSNNESE TFR	>50	>50	0.3	>50	0.04	0.7	10.4	1616
T278-50.Loop D mut/V5 Swap	NISDNAKT	TKPSGGDLEITTH	GGNSNNESE TFR	0.65	4.1	0.03	>50	0.004	0.1	6.0	>5000
BL01.WT	NFTQNAET	NPPIRGGDPEIVMH	GGKNGTEGTE IFR	>50	>50	0.1	1.7	0.01	0.4	0.7	738
BL01.V5 Swap	NFTQNAET	NPPIRGGDPEIVMH	GGKNESEIE IFR	>50	>50	0.1	9.4	0.016	0.1	0.03	801
BL01.Loop D/V5 Swap	NFTDNAKT	NPPIRGGDPEIVMH	GGKNESEIE IFR	6.3	>50	0.1	8.7	0.008	0.1	0.5	755
BL01.Loop D/CD4 BLP mut/V5 Swap	NFTDNAKT	KQSSGGDPEIVMH	GGKNESEIE IFR	0.084	0.49	0.001	0.41	0.002	0.04	0.13	5000
TV1_29.WT	NLTENTKT	KPHAGGDIEITMH	GGFNTTNNTE TFR	>50	>50	>50	>50	19.0	0.2	4.5	1013
TV1_29.V5 Swap	NLTENTKT	KPHAGGDIEITMH	GGKNESEI E TFR	ND	>50	ND	>50	ND	0.5	ND	1583
TV1_29.Loop D mut/V5 Swap	NLTDNAKT	KPHAGGDIEITMH	GGKNESEI E TFR	1.82	11.6	>50	>50	0.026	2.3	0.080	239
TV1_29.Loop D/CD4 BLP mut/V5 Swap	NLTDNAKT	KQSSGGDIEITMH	GGKNESEI E TFR	0.59	2.2	0.0398	>50	0.024	3.5	0.087	480
57128_02.WT	NLTNNAKI	NASSGGDLEITTH	GGGADNNRQNE TFR	8.7	>50	0.002	0.192	0.04	0.16	0.4	413
57128_02.WT.Kif treated	NLTNNAKI	NASSGGDLEITTH	GGGADNNRQNE TFR	ND	>50	ND	1.82	ND	0.27	ND	548
57128_02.Loop D mut/V5 Swap	NLTNNAKT	NASSGGDLEITTH	GGNSNNESE IFR	ND	17.8	ND	0.22	ND	0.45	ND	2016
57128_02.Loop D mut/V5 Swap. Kif treated	NLTNNAKT	NASSGGDLEITTH	GGNSNNESE IFR	ND	15.4	ND	1.6	ND	1.40	ND	901
57128_02.Loop D/CD4 BLP mut/V5 Swap	NLTNNAKT	KQSSGGDLEITTH	GGNSNNESE IFR	0.049	7.4	0.0006	0.04	1.31	0.68	0.061	1070
3817_V2_C59.WT	NVTNNAKT	SPSSGGDPEITTH	GGLNTSNNE TFR	0.04	>50	0.003	>50	0.001	>50	0.06	>5000
3817_V2_C59.WT.Kif treated	NVTNNAKT	SPSSGGDPEITTH	GGLNTSNNE TFR	ND	3.3	ND	>50	ND	>50	ND	433

<1ug/ml
1-50 ug/ml
>50ug/ml

[a] B-EC$_{50}$ (μg/ml), half-maximal effective concentration of ELISA binding assay.
[b] N-IC$_{50}$ (μg/ml), 50% inhibitory concentration of neutralization assay.
[c] Three VRC01-sensitive virus gp120 sequences are listed at top as references. VRC01-resistant virus gp120 variations from the reference sequences are listed in bold red type. The mutated residues are marked in bold black type and underlined.

enhanced binding to gp120 in the presence of both CD4-Ig and VRC01 (Fig. 5C). Similarly the CD4i MAb A32, which binds to the gp120 C1-to-C4 region (46), rather than the coreceptor binding region, also displayed enhanced recognition of gp120 in the presence of VRC01 (Fig. 5C). In contrast, 2.1C, a CD4i antibody whose epitope overlaps with coreceptor binding site, displayed enhanced binding in the presence of CD4-Ig; however, its binding to gp120 was decreased in the presence of VRC01 (Fig. 5C). This is consistent with the fact that both VRC01 and 2.1C appear to interact with residue V430 on gp120 (15, 73) and likely have overlapping epitopes. Despite this single exception, the interaction of VRC01 with monomeric gp120 in the antibody induction context appears to be similar to that of CD4.

VRC01 and CD4 have markedly different effects on the functional Env spike. While VRC01 and CD4-Ig have similar effects on monomeric gp120, the Ala scanning of gp120 in the context of the functional viral spike revealed distinct differences between VRC01 and CD4-Ig interactions. Therefore, we sought to analyze additional interactions of these ligands with gp120 in the context of the functional spike. It was shown previously that *in vitro*, upon addition of sCD4 to Env-expressing cells or to free virus, the gp120 subunit dissociates from gp41 and is "shed" from the spike into the surrounding tissue culture media (6, 26, 44, 45, 48) (so-called "CD4-induced shedding"). To investigate if VRC01 can similarly induce shedding of gp120 from the functional trimer *in vitro*, we transfected 293T cells with plasmids encoding the JRCSF or JRFL Env to generate HIV-1 trimers on the surface of these cells. Following transient expression, sCD4 or VRC01 was added to the trimer-displaying cells, and immune-precipitation using the anti-V3 antibody 39F was performed to detect any gp120 that was shed into the supernatant. The shed, monomeric gp120 was resolved by SDS-PAGE gels and quantified by Western blotting (Fig. 6A). As expected, sCD4 induced significant gp120 shedding from both the cell surface JRFL and JRCSF Env trimers, in a dose-dependent manner. However, there was no measurable shedding of gp120 induced by the VRC01 MAb. Interestingly, although MAb b12 induces little conformational change to gp120 as assessed by thermodynamic analysis (34, 74), it induced gp120 shedding from JRFL cell surface Env trimers (Fig. 6A). The lack of VRC01-induced gp120 shedding, even in the context of the labile JRFL cell surface Env spike, implies that VRC01 interacts with the functional virus spike in a man-

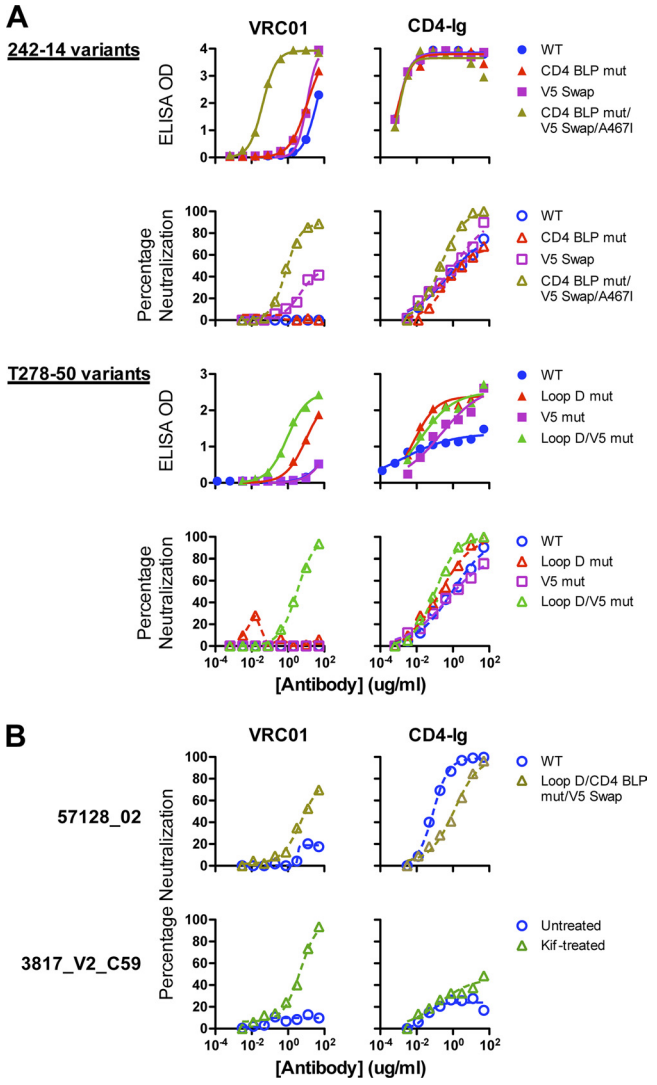

FIG. 4. Binding and neutralization of reversion mutants and chimeras of VRC01-resistant viruses. (A) VRC01-resistant viruses 242-14 and T278-50 and their reversion mutants. Curves show binding and neutralization with VRC01 or CD4-Ig. The specific reversion mutants and chimeras are described in Table 2. (B) Analysis of two Env pseudoviruses that were resistant to VRC01 despite recognition of the viral gp120. gp120 of virus 57128_02 bound to VRC01 with an EC_{50} of 8.7 μg/ml (Table 1) yet was resistant to VRC01 neutralization. With additional reversion mutations in loop D, CD4 binding loop, and V5, the mutant virus was moderately neutralized by VRC01 (top). Virus 3817_V2_C59 was resistant to VRC01 neutralization (bottom) despite strong recognition of its gp120 by VRC01 (EC_{50} of 0.04 μg/ml, Table 1). When the virus was produced in the presence of the glycan modification inhibitor kifunensin, it became sensitive to VRC01-mediated neutralization (bottom).

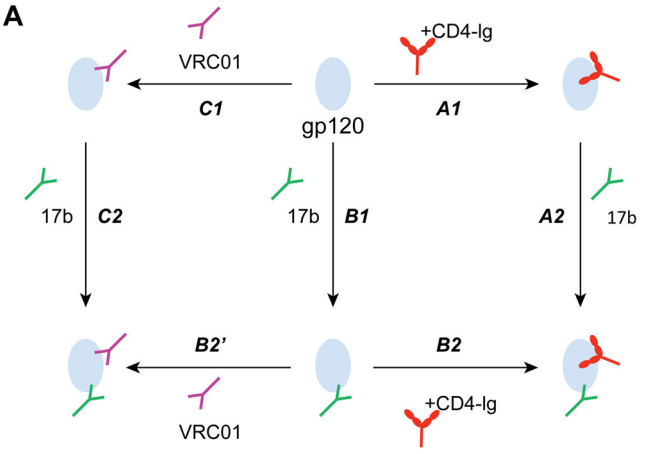

B

	Interaction	ΔH (kcal/mol)	-TΔS (kcal/mol)	ΔG (kcal/mol)
A1	YU2gp120 + CD4-Ig*	-50.75±1.38	40.03±0.81	-10.72±0.85
C1	YU2gp120 + VRC01*	-48.6±1.29	38.73±0.65	-9.87±0.18
B1	YU2gp120 + 17b	-47.16±1.23	37.43±0.62	-9.73±0.12
A2	(YU2gp120 + CD4-Ig) + 17b	-17.99±0.54	7.52±0.54	-10.47±0.94
C2	(YU2gp120 + VRC01) + 17b	-25.28±0.65	15.03±0.34	-10.25±0.16
B2	(YU2gp120 + 17b) + CD4 -Ig	-26.08±0.68	16.17±0.35	-9.91±0.17
B2'	(YU2gp120 + 17b) + VRC01	-31.27±0.84	21.58±0.43	-9.69±0.17

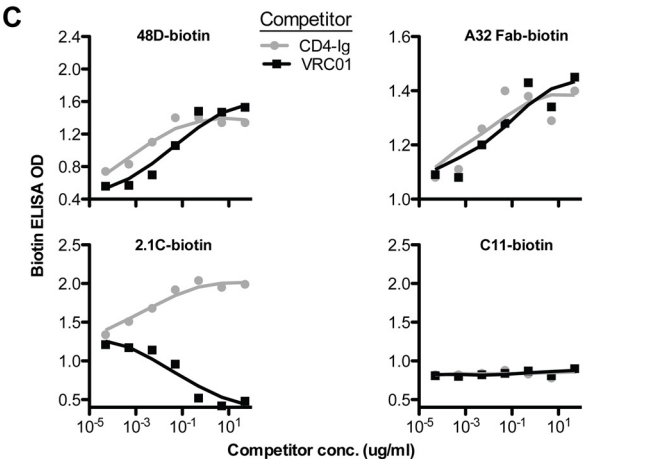

FIG. 5. VRC01 effects on monomeric gp120, compared with CD4-Ig. (A) Scheme of thermodynamic cycles showing enhancement of binding to gp120 between CD4bs ligands CD4-Ig and VRC01 and the CD4i antibody 17b. (B) Thermodynamic values of CD4-Ig, VRC01, and 17b interactions with gp120 measured by ITC at 37°C, including the change in enthalpy (ΔH) and entropy ($-T\Delta S$) upon binding of gp120 to the coreceptor mimetic antibody 17b, antibody VRC01, and CD4-Ig, a surrogate for the primary receptor, CD4. *, data extracted from reference 70. (C) Effect on other CD4i antibodies binding to gp120, captured by sheep anti-gp120 C5 antibody D7324 on ELISA plate. The binding of biotin-labeled CD4i antibodies, 48D, A32 Fab, and 2.1C to gp120 was tested in the presence of CD4-Ig or VRC01, with signals detected by the streptavidin-HRP conjugate. The MAb C11, which recognizes a C1-to-C5 conformational epitope on gp120, was used as negative control.

ner that causes less alteration of the configuration of the viral Env spike than does either CD4 or the MAb b12.

To further investigate this apparent difference between MAbs VRC01 and sCD4 in their respective interaction with gp120 in the context of the trimeric spike, we assessed the effects on the gp41 subunit following incubation of these two CD4 binding site ligands. The rationale for this experiment is as follows. As a key functional component of the functional spike, gp41 undergoes significant rearrangement after gp120 engages CD4 (and perhaps the coreceptor CCR5) to mediate viral entry. The membrane proximal external region (MPER) is a highly conserved and important functional region of gp41 and is the target of the broadly neutralizing antibodies 2F5 and 4E10. The MPER of primary isolates has been demonstrated

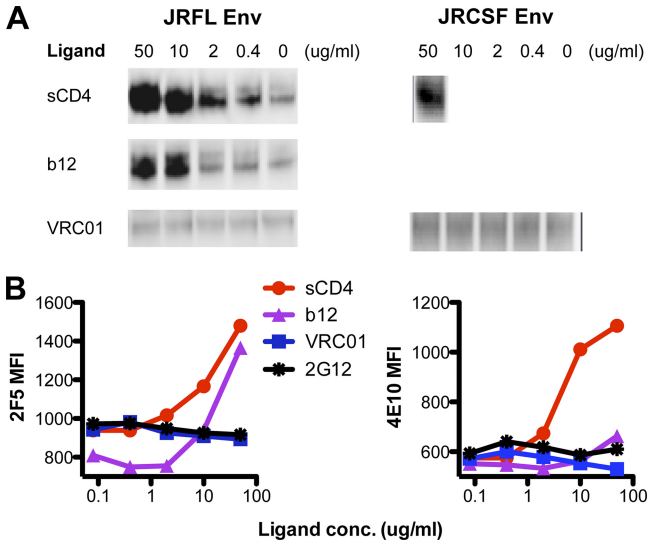

FIG. 6. VRC01 effects on HIV envelope glycoprotein functional trimer. (A) Western blot analysis of Env from supernatants of 293T cells transfected with cleavage competent gp160 JRFL or JRCSF Env plasmid DNA. HIV-1 gp120 shedding upon binding of ligands, including sCD4, b12, and VRC01, from the Env trimer on the surface of 293T cells was evaluated by probing the blot with the anti-gp120 human monoclonal antibody 39F (V3 specific). (B) Effect of VRC01, b12, and sCD4 on gp41 MPER-directed antibodies 2F5 and 4E10 binding to trimeric Env. 293T cells transfected with JRFL-ΔCT Env expression plasmid were stained with biotin-labeled 2F5 or 4E10. Binding of 2F5 or 4E10 to JRFL Env in the presence of the CD4bs ligands VRC01, b12, and sCD4 was detected with streptavidin-APC conjugate. MFI, mean fluorescence intensity.

to be occluded on the envelope trimer prior to receptor engagement (9, 76) and becomes more accessible to 2F5 or 4E10 after CD4 binding (9, 53), presumably by substantial conformational changes induced in the overall Env spike architecture by CD4 interaction with the gp120 subunit, which is intimately associated with the gp41 subunit. To investigate the effect of VRC01 on accessibility of the gp41 MPER to antibody, we assessed 2F5 or 4E10 binding to JRFL Env-expressing cells in the presence, or absence, of the CD4bs ligand subset of VRC01, b12, and sCD4. Consistent with our prior findings and the shedding data presented here, both sCD4 and b12 enhanced 2F5 binding to the Env functional trimer (9) (Fig. 6B). In contrast, VRC01 had no effect on 2F5 binding to the functional spike (Fig. 6B), similar to the negligible effects on MPER recognition induced by the glycan-dependent negative-control antibody 2G12. Similarly, preincubation of sCD4 with the JRFL Env-expressing cells enhanced recognition of cell surface Env by the other MPER-directed neutralizing MAb, 4E10 (Fig. 6B). Preincubation of the cell surface Env with b12 slightly enhanced 4E10 binding, but VRC01 had no effect. These data again suggest that unlike CD4, binding by VRC01 to gp120 does not induce conformational changes in the context of the functional spike. Thus, although the conformational signatures of VRC01 and CD4 are very similar on the soluble gp120 monomer, they have distinctly different signatures on the architecture of the viral functional spike.

Lack of self-reactivity or polyreactivity. VRC01 was also tested for evidence of self- or polyreactivity. We observed no evidence of VRC01 binding to human HEp-2 epithelial cells, which are often used for the detection and identification of antinuclear antibodies (27) (Fig. 7A). VCR01 also displayed little or no reactivity by the Luminex assay to a diverse panel of autoantigens (Fig. 7B) and no reactivity by ELISA to cardiolipin (not shown). Lastly, VRC01 was tested for antiphospholipid activity using the clinical activated partial thromboplastin test (aPTT). No prolongation of the clotting time was observed for VRC01 (Fig. 7C), indicating that VRC01 does not have significant antiphospholipid binding properties.

DISCUSSION

In this study, we assessed the interaction of the broadly neutralizing MAb VRC01 with the HIV-1 native viral spike, and where informative, to full-length monomeric gp120. We measured the effect of gp120 Ala scanning point mutations on virus neutralization and recognition of gp120 by VRC01 and the prototypic CD4bs ligands b12 and CD4-Ig. We also analyzed the contribution of amino acid variation within specific regions of Env to viral resistance to VRC01. In addition, we compared the thermodynamic properties of VRC01 and CD4-Ig (or sCD4) and assessed their impact on the conformation of gp120 and the native viral spike. Finally, we determined that there was little detectable interaction of the human MAb VRC01 with human antigens commonly recognized by self-reactive antibodies that may have escaped the normal regulatory mechanisms of B-cell self-tolerance.

There are several important findings highlighted by the results presented in our current study. We confirmed that mutations of structurally defined contact residues in loop D (N terminal to the V3 region), the CD4 binding loop, and the V5-β24-α5 region diminished VRC01-mediated binding or neutralization. With regard to natural resistance, in most cases, combinations of mutations at these sites were required to restore full VRC01 neutralization sensitivity. Interestingly, many Ala substitutions at noncontact residues increased the potency of CD4- or b12-mediated neutralization, but few of these substitutions enhanced VRC01-mediated neutralization. This suggests that VRC01 targets its epitope on the functional spike in a highly precise manner, overcoming the steric constraints that restrict the binding of many Env ligands. The observation that VRC01 targeting appears to be superior to the primary virus receptor itself is somewhat paradoxical, as one might expect that HIV-1 would maintain optimal recognition of its primary receptor, CD4. We speculate that selective pressure imposed by CD4 binding site antibodies may select for viruses that occlude optimal access to the CD4 binding region, even for CD4 itself. Obviously, the favorable energetics of the CD4-gp120 interaction allow the viral spike to engage host cell CD4, triggering the conformational changes in Env necessary for viral entry. In contrast, the relatively uncommon CD4bs ligand, VRC01, appears to target the functional spike in a manner that requires limited Env spike rearrangement to accomplish access and neutralization. The lack of VRC01-induced gp120 shedding and the lack of conformational changes of the native virus spike observed after VRC01 binding are consistent with this interpretation. Somewhat paradoxically, VRC01-induced conformational changes on the free gp120 monomer generated a signature that was very similar to that of CD4, implying that

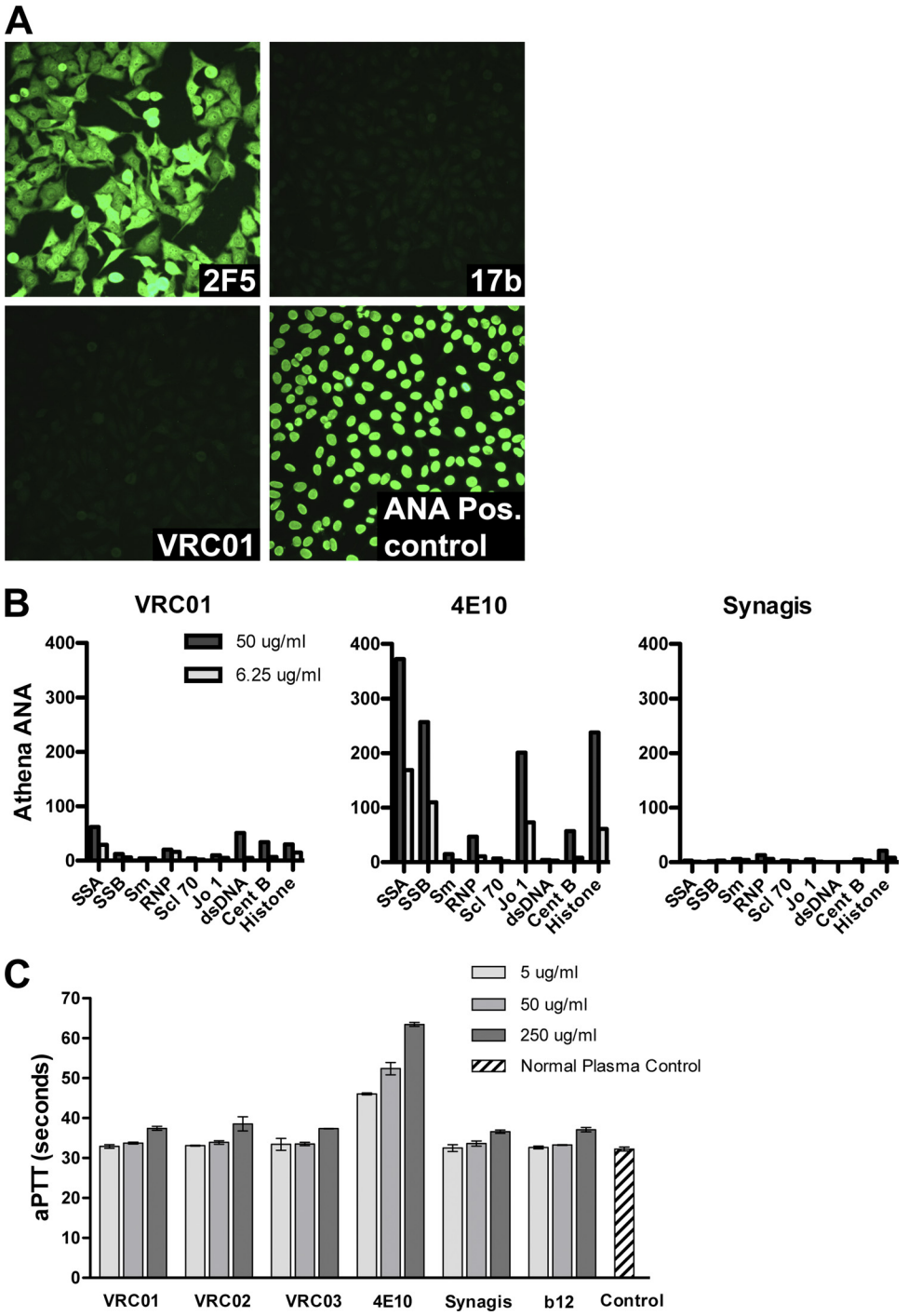

FIG. 7. Lack of VRC01 self-reactivity. (A) Reactivity of MAbs 2F5, 17b, and VRC01 with human HEp-2 epithelial cells. The MAb 2F5 served as a positive control and reacted in a diffuse cytoplasmic and nuclear pattern. (B) Luminex AtheNA Multi-Lyte ANA test for a panel of nuclear antigens: systemic lupus erythematosus autoantigens SSA and SSB, sphingomyelin (Sm), ribonucleoprotein (RNP), sclerosis autoantigen (Scl-70), histidine-tRNA ligase (Jo-1), double-stranded DNA (dsDNA), and centromere B (CentB). (C) The clinical assay, activated partial thromboplastin time (aPTT), was used to assess potential antiplatelet, antiphospholipid activity. The MAbs were added to normal sera, and the time to clot formation was measured. The clotting times for VRC01, VRC02, VRC03, b12, and the anti-RSV monoclonal antibody Synagis (palivizumab) were all in the normal range. In contrast, the known polyreactive MAb 4E10 caused a prolongation of the aPTT.

the conformation of free gp120 is considerably different than its conformation on the functional spike. Alternatively, VRC01 may indeed induce conformational changes on the functional trimer that are not detected by the assays used in this study but that serve to constrain gp120 in a (low-energy) state not compatible with coreceptor interaction or liberation of the gp41 fusion peptide required for entry.

Our studies of the mechanism of neutralization resistance to

VRC01 reveal that a minority of viruses do contain alterations in key contact sites that diminish VRC01 binding and neutralization. However, we found only one example of a viral isolate that appears to resist VRC01 neutralization by restricting the antibodies' access to the CD4bs. These observations are consistent with the model in which VRC01 has achieved nearly optimal access to the CD4bs on the functional spike (70, 73). We further defined specific aspects of neutralization resistance among a panel of 16 VRC01-resistant Env pseudoviruses. We demonstrated that full VRC01 neutralization sensitivity could be restored to several viruses possessing natural escape variations in their respective Envs. However, restoration of VRC01 sensitivity was accomplished only after multiple changes in three gp120 hotspots, suggesting that viral resistance might require multiple, and perhaps sequential, alterations. Ongoing studies will evaluate the effect of these VRC01 resistance mutations on the efficiency of CD4-mediated cell entry and on viral replicative fitness.

In our previous study, we reported that VRC01 could enhance CD4i antibody 17b and coreceptor CCR5 binding to monomeric gp120 (70). In the current study, we extended such analysis and observed similarly that the binding of other CD4i antibodies to gp120 was enhanced by prior VRC01 interaction, a property similar to that of CD4. However, when we compared the effects of VRC01 to sCD4 interaction in the context of the functional trimer by other means of analysis, again there were striking differences from the monomeric context. We found that sCD4 binding to the functional trimer can trigger gp120 shedding from the Env trimer and enhancement of gp41 MPER exposure, confirming previous work that CD4 can induce substantial rearrangements of the functional spike, likely necessary to permit entry. In contrast, we did not see the induction of gp120 shedding or enhancement of gp41 MPER exposure after VRC01 bound to the Env functional trimer. These data support a model in which VRC01 locks the Env functional trimer into a low-energy conformation (or trough) from which it cannot "escape" to undergo the further rearrangements that eventually coalesce in virus entry. Finally, the observation that VRC01 does not display substantial self-reactive or polyreactive properties will facilitate the use of passive protection studies of nonhuman primates and humans. This outcome is perhaps not so surprising since VRC01, as noted previously, does not possess an exceptionally long or hydrophobic HCDR3 loop (28), both of which have correlated with some level of self-reactivity previously.

In summary, the data presented here support the concept that VRC01 interacts with the functional spike in a manner distinct from that of CD4. VRC01 achieves potent neutralization by precisely targeting a highly conserved region of the CD4bs without requiring the alterations of the Env functional spike configuration that occur upon CD4 ligation. This helps to explain how VRC01 can access the CD4bs on the large majority of virus isolates and why VRC01 resistance based on the quaternary structure of the HIV-1 Env is uncommon. These studies highlight the unique features of this broadly neutralizing CD4bs-directed antibody and point to further efforts regarding HIV immunogen design based on its gp120 epitope.

ACKNOWLEDGMENTS

We are grateful to Christian Poulsen for help with molecular modeling, Christina Corbaci for help with manuscript preparation, James Robinson (Tulane University) for providing antibodies, including C11, 17b, 48D, 2.1c, and A32, Susan Zolla-Pazner (New York University) for providing antibody 447D, and Joseph Sodroski (Dana Farber Cancer Institute) for providing the plasmid encoding CD4-Ig.

This study was supported by the Intramural Research Program of the Vaccine Research Center, National Institute of Allergy and Infectious Diseases, National Institutes of Health, and the International AIDS Vaccine Initiative.

REFERENCES

1. **Alkhatib, G., et al.** 1996. CC CKR5: a RANTES, MIP-1alpha, MIP-1beta receptor as a fusion cofactor for macrophage-tropic HIV-1. Science **272:** 1955–1958.
2. **Binley, J. M., et al.** 2010. Role of complex carbohydrates in human immunodeficiency virus type 1 infection and resistance to antibody neutralization. J. Virol. **84:**5637–5655.
3. **Binley, J. M., et al.** 2008. Profiling the specificity of neutralizing antibodies in a large panel of plasmas from patients chronically infected with human immunodeficiency virus type 1 subtypes B and C. J. Virol. **82:**11651–11668.
4. **Blish, C. A., M. A. Nguyen, and J. Overbaugh.** 2008. Enhancing exposure of HIV-1 neutralization epitopes through mutations in gp41. PLoS Med. **5:**e9.
5. **Buchacher, A., et al.** 1994. Generation of human monoclonal antibodies against HIV-1 proteins; electrofusion and Epstein-Barr virus transformation for peripheral blood lymphocyte immortalization. AIDS Res. Hum. Retroviruses **10:**359–369.
6. **Bugelski, P. J., H. Ellens, T. K. Hart, and R. L. Kirsh.** 1991. Soluble CD4 and dextran sulfate mediate release of gp120 from HIV-1: implications for clinical trials. J. Acquir. Immune Defic. Syndr. **4:**923–924.
7. **Burton, D. R., et al.** 1994. Efficient neutralization of primary isolates of HIV-1 by a recombinant human monoclonal antibody. Science **266:**1024–1027.
8. **Calarese, D. A., et al.** 2005. Dissection of the carbohydrate specificity of the broadly neutralizing anti-HIV-1 antibody 2G12. Proc. Natl. Acad. Sci. U. S. A. **102:**13372–13377.
9. **Chakrabarti, B. K., et al.** 2011. HIV type 1 Env precursor cleavage state affects recognition by both neutralizing and nonneutralizing gp41 antibodies. AIDS Res. Hum. Retroviruses [Epub ahead of print.] doi:10.1089/aid.2010.0281.
10. **Chan, D. C., D. Fass, J. M. Berger, and P. S. Kim.** 1997. Core structure of gp41 from the HIV envelope glycoprotein. Cell **89:**263–273.
11. **Choe, H., et al.** 1996. The beta-chemokine receptors CCR3 and CCR5 facilitate infection by primary HIV-1 isolates. Cell **85:**1135–1148.
12. **Dalgleish, A. G., et al.** 1984. The CD4 (T4) antigen is an essential component of the receptor for the AIDS retrovirus. Nature **312:**763–767.
13. **Deng, H., et al.** 1996. Identification of a major co-receptor for primary isolates of HIV-1. Nature **381:**661–666.
14. **Dhillon, A. K., et al.** 2007. Dissecting the neutralizing antibody specificities of broadly neutralizing sera from human immunodeficiency virus type 1-infected donors. J. Virol. **81:**6548–6562.
15. **Diskin, R., P. M. Marcovecchio, and P. J. Bjorkman.** 2010. Structure of a clade C HIV-1 gp120 bound to CD4 and CD4-induced antibody reveals anti-CD4 polyreactivity. Nat. Struct. Mol. Biol. **17:**608–613.
16. **Doores, K. J., and D. R. Burton.** 2010. Variable loop glycan dependency of the broad and potent HIV-1-neutralizing antibodies PG9 and PG16. J. Virol. **84:**10510–10521.
17. **Doranz, B. J., et al.** 1996. A dual-tropic primary HIV-1 isolate that uses fusin and the beta-chemokine receptors CKR-5, CKR-3, and CKR-2b as fusion cofactors. Cell **85:**1149–1158.
18. **Doria-Rose, N. A., et al.** 2010. Breadth of human immunodeficiency virus-specific neutralizing activity in sera: clustering analysis and association with clinical variables. J. Virol. **84:**1631–1636.
19. **Dragic, T., et al.** 1996. HIV-1 entry into CD4+ cells is mediated by the chemokine receptor CC-CKR-5. Nature **381:**667–673.
20. **Earl, P. L., et al.** 1994. Native oligomeric human immunodeficiency virus type 1 envelope glycoprotein elicits diverse monoclonal antibody reactivities. J. Virol. **68:**3015–3026.
21. **Earl, P. L., R. W. Doms, and B. Moss.** 1990. Oligomeric structure of the human immunodeficiency virus type 1 envelope glycoprotein. Proc. Natl. Acad. Sci. U. S. A. **87:**648–652.
22. **Feng, Y., C. C. Broder, P. E. Kennedy, and E. A. Berger.** 1996. HIV-1 entry cofactor: functional cDNA cloning of a seven-transmembrane, G protein-coupled receptor. Science **272:**872–877.
23. **Furuta, R. A., C. T. Wild, Y. Weng, and C. D. Weiss.** 1998. Capture of an early fusion-active conformation of HIV-1 gp41. Nat. Struct. Biol. **5:**276–279.
24. **Gray, E. S., et al.** 2007. Neutralizing antibody responses in acute human immunodeficiency virus type 1 subtype C infection. J. Virol. **81:**6187–6196.
25. **Gray, E. S., et al.** 2009. Antibody specificities associated with neutralization

breadth in plasma from human immunodeficiency virus type 1 subtype C-infected blood donors. J. Virol. **83:**8925–8937.
26. **Hart, T. K., et al.** 1991. Binding of soluble CD4 proteins to human immunodeficiency virus type 1 and infected cells induces release of envelope glycoprotein gp120. Proc. Natl. Acad. Sci. U. S. A. **88:**2189–2193.
27. **Haynes, B. F., et al.** 2005. Cardiolipin polyspecific autoreactivity in two broadly neutralizing HIV-1 antibodies. Science **308:**1906–1908.
28. **Haynes, B. F., M. A. Moody, L. Verkoczy, G. Kelsoe, and S. M. Alam.** 2005. Antibody polyspecificity and neutralization of HIV-1: a hypothesis. Hum. Antibodies **14:**59–67.
29. **He, Y., et al.** 2003. Peptides trap the human immunodeficiency virus type 1 envelope glycoprotein fusion intermediate at two sites. J. Virol. **77:**1666–1671.
30. **Klatzmann, D., et al.** 1984. T-lymphocyte T4 molecule behaves as the receptor for human retrovirus LAV. Nature **312:**767–768.
31. **Koch, M., et al.** 2003. Structure-based, targeted deglycosylation of HIV-1 gp120 and effects on neutralization sensitivity and antibody recognition. Virology **313:**387–400.
32. **Kolchinsky, P., E. Kiprilov, and J. Sodroski.** 2001. Increased neutralization sensitivity of CD4-independent human immunodeficiency virus variants. J. Virol. **75:**2041–2050.
33. **Koshiba, T., and D. C. Chan.** 2003. The prefusogenic intermediate of HIV-1 gp41 contains exposed C-peptide regions. J. Biol. Chem. **278:**7573–7579.
34. **Kwong, P. D., et al.** 2002. HIV-1 evades antibody-mediated neutralization through conformational masking of receptor-binding sites. Nature **420:**678–682.
35. **Li, M., et al.** 2005. Human immunodeficiency virus type 1 env clones from acute and early subtype B infections for standardized assessments of vaccine-elicited neutralizing antibodies. J. Virol. **79:**10108–10125.
36. **Li, Y., et al.** 2008. Removal of a single N-linked glycan in human immunodeficiency virus type 1 gp120 results in an enhanced ability to induce neutralizing antibody responses. J. Virol. **82:**638–651.
37. **Li, Y., et al.** 2007. Broad HIV-1 neutralization mediated by CD4-binding site antibodies. Nat. Med. **13:**1032–1034.
38. **Li, Y., et al.** 2009. Analysis of neutralization specificities in polyclonal sera derived from human immunodeficiency virus type 1-infected individuals. J. Virol. **83:**1045–1059.
39. **Liu, J., A. Bartesaghi, M. J. Borgnia, G. Sapiro, and S. Subramaniam.** 2008. Molecular architecture of native HIV-1 gp120 trimers. Nature **455:**109–113.
40. **Lu, M., S. C. Blacklow, and P. S. Kim.** 1995. A trimeric structural domain of the HIV-1 transmembrane glycoprotein. Nat. Struct. Biol. **2:**1075–1082.
41. **Mascola, J. R., and D. C. Montefiori.** 2010. The role of antibodies in HIV vaccines. Annu. Rev. Immunol. **28:**413–444.
42. **McDougal, J. S., et al.** 1986. Binding of HTLV-III/LAV to T4+ T cells by a complex of the 110K viral protein and the T4 molecule. Science **231:**382–385.
43. **Moog, C., H. J. Fleury, I. Pellegrin, A. Kirn, and A. M. Aubertin.** 1997. Autologous and heterologous neutralizing antibody responses following initial seroconversion in human immunodeficiency virus type 1-infected individuals. J. Virol. **71:**3734–3741.
44. **Moore, J. P., J. A. McKeating, W. A. Norton, and Q. J. Sattentau.** 1991. Direct measurement of soluble CD4 binding to human immunodeficiency virus type 1 virions: gp120 dissociation and its implications for virus-cell binding and fusion reactions and their neutralization by soluble CD4. J. Virol. **65:**1133–1140.
45. **Moore, J. P., J. A. McKeating, R. A. Weiss, and Q. J. Sattentau.** 1990. Dissociation of gp120 from HIV-1 virions induced by soluble CD4. Science **250:**1139–1142.
46. **Moore, J. P., and J. Sodroski.** 1996. Antibody cross-competition analysis of the human immunodeficiency virus type 1 gp120 exterior envelope glycoprotein. J. Virol. **70:**1863–1872.
47. **Myszka, D. G., et al.** 2000. Energetics of the HIV gp120-CD4 binding reaction. Proc. Natl. Acad. Sci. U. S. A. **97:**9026–9031.
48. **Orloff, S. L., M. S. Kennedy, A. A. Belperron, P. J. Maddon, and J. S. McDougal.** 1993. Two mechanisms of soluble CD4 (sCD4)-mediated inhibition of human immunodeficiency virus type 1 (HIV-1) infectivity and their relation to primary HIV-1 isolates with reduced sensitivity to sCD4. J. Virol. **67:**1461–1471.
49. **Pancera, M., and R. Wyatt.** 2005. Selective recognition of oligomeric HIV-1 primary isolate envelope glycoproteins by potently neutralizing ligands requires efficient precursor cleavage. Virology **332:**145–156.
50. **Pantophlet, R., and D. R. Burton.** 2006. GP120: target for neutralizing HIV-1 antibodies. Annu. Rev. Immunol. **24:**739–769.
51. **Pantophlet, R., et al.** 2003. Fine mapping of the interaction of neutralizing and nonneutralizing monoclonal antibodies with the CD4 binding site of human immunodeficiency virus type 1 gp120. J. Virol. **77:**642–658.
52. **Parker, C. E., et al.** 2001. Fine definition of the epitope on the gp41 glycoprotein of human immunodeficiency virus type 1 for the neutralizing monoclonal antibody 2F5. J. Virol. **75:**10906–10911.
53. **Peachman, K. K., L. Wieczorek, V. R. Polonis, C. R. Alving, and M. Rao.** 2010. The effect of sCD4 on the binding and accessibility of HIV-1 gp41 MPER epitopes to human monoclonal antibodies. Virology **408:**213–223.
54. **Pinter, A., et al.** 1989. Oligomeric structure of gp41, the transmembrane protein of human immunodeficiency virus type 1. J. Virol. **63:**2674–2679.
55. **Richman, D. D., T. Wrin, S. J. Little, and C. J. Petropoulos.** 2003. Rapid evolution of the neutralizing antibody response to HIV type 1 infection. Proc. Natl. Acad. Sci. U. S. A. **100:**4144–4149.
56. **Sanders, R. W., et al.** 2002. The mannose-dependent epitope for neutralizing antibody 2G12 on human immunodeficiency virus type 1 glycoprotein gp120. J. Virol. **76:**7293–7305.
57. **Sather, D. N., et al.** 2009. Factors associated with the development of cross-reactive neutralizing antibodies during human immunodeficiency virus type 1 infection. J. Virol. **83:**757–769.
58. **Scanlan, C. N., et al.** 2002. The broadly neutralizing anti-human immunodeficiency virus type 1 antibody 2G12 recognizes a cluster of alpha1→2 mannose residues on the outer face of gp120. J. Virol. **76:**7306–7321.
59. **Scanlan, C. N., et al.** 2007. Inhibition of mammalian glycan biosynthesis produces non-self antigens for a broadly neutralising, HIV-1 specific antibody. J. Mol. Biol. **372:**16–22.
60. **Si, Z., et al.** 2004. Small-molecule inhibitors of HIV-1 entry block receptor-induced conformational changes in the viral envelope glycoproteins. Proc. Natl. Acad. Sci. U. S. A. **101:**5036–5041.
61. **Simek, M. D., et al.** 2009. Human immunodeficiency virus type 1 elite neutralizers: individuals with broad and potent neutralizing activity identified by using a high-throughput neutralization assay together with an analytical selection algorithm. J. Virol. **83:**7337–7348.
62. **Stamatatos, L., L. Morris, D. R. Burton, and J. R. Mascola.** 2009. Neutralizing antibodies generated during natural HIV-1 infection: good news for an HIV-1 vaccine? Nat. Med. **15:**866–870.
63. **Trkola, A., et al.** 1996. CD4-dependent, antibody-sensitive interactions between HIV-1 and its co- receptor CCR-5. Nature **384:**184–187.
64. **Trkola, A., et al.** 1996. Human monoclonal antibody 2G12 defines a distinctive neutralization epitope on the gp120 glycoprotein of human immunodeficiency virus type 1. J. Virol. **70:**1100–1108.
65. **Walker, L. M., et al.** 2009. Broad and potent neutralizing antibodies from an African donor reveal a new HIV-1 vaccine target. Science **326:**285–289.
66. **Wei, X., et al.** 2003. Antibody neutralization and escape by HIV-1. Nature **422:**307–312.
67. **Weiss, C. D., J. A. Levy, and J. M. White.** 1990. Oligomeric organization of gp120 on infectious human immunodeficiency virus type 1 particles. J. Virol. **64:**5674–5677.
68. **Weissenhorn, W., A. Dessen, S. C. Harrison, J. J. Skehel, and D. C. Wiley.** 1997. Atomic structure of the ectodomain from HIV-1 gp41. Nature **387:**426–430.
69. **Wu, L., et al.** 1996. CD4-induced interaction of primary HIV-1 gp120 glycoproteins with the chemokine receptor CCR-5. Nature **384:**179–183.
70. **Wu, X., et al.** 2010. Rational design of envelope identifies broadly neutralizing human monoclonal antibodies to HIV-1. Science **329:**856–861.
71. **Wu, X., et al.** 2009. Mechanism of human immunodeficiency virus type 1 resistance to monoclonal antibody B12 that effectively targets the site of CD4 attachment. J. Virol. **83:**10892–10907.
72. **Wyatt, R., and J. Sodroski.** 1998. The HIV-1 envelope glycoproteins: fusogens, antigens, and immunogens. Science **280:**1884–1888.
73. **Zhou, T., et al.** 2010. Structural basis for broad and potent neutralization of HIV-1 by antibody VRC01. Science **329:**811–817.
74. **Zhou, T., et al.** 2007. Structural definition of a conserved neutralization epitope on HIV-1 gp120. Nature **445:**732–737.
75. **Zwick, M. B., et al.** 2005. Anti-human immunodeficiency virus type 1 (HIV-1) antibodies 2F5 and 4E10 require surprisingly few crucial residues in the membrane-proximal external region of glycoprotein gp41 to neutralize HIV-1. J. Virol. **79:**1252–1261.
76. **Zwick, M. B., et al.** 2001. Broadly neutralizing antibodies targeted to the membrane-proximal external region of human immunodeficiency virus type 1 glycoprotein gp41. J. Virol. **75:**10892–10905.